THE JOURNAL OF BIOLOGICAL CHEMISTRY VOL. 288, NO. 5, pp. 3174–3183, February 1, 2013
© 2013 by The American Society for Biochemistry and Molecular Biology, Inc. Published in the U.S.A.

PHF6 Regulates Cell Cycle Progression by Suppressing Ribosomal RNA Synthesis*

Received for publication, August 29, 2012, and in revised form, December 8, 2012 Published, JBC Papers in Press, December 10, 2012, DOI 10.1074/jbc.M112.414839

Jiadong Wang[‡], Justin Wai-chung Leung[‡], Zihua Gong[‡], Lin Feng[‡], Xiaobing Shi[§], and Junjie Chen[‡1]

From the [‡]Department of Experimental Radiation Oncology and the [§]Department of Biochemistry and Molecular Biology, University of Texas M.D. Anderson Cancer Center, Houston, Texas 77030

Background: PHF6 is mutated in T-cell acute lymphoblastic leukemias.
Results: Knockdown of PHF6 impairs cell proliferation, arrests cells at G_2/M phase, and increases rRNA transcription and DNA damage at the rDNA locus.
Conclusion: PHF6 regulates cell cycle progression by suppressing ribosomal RNA synthesis.
Significance: The tumor suppressor function of PHF6 may be linked with its roles in regulating rRNA synthesis and genome maintenance.

Mutation of PHF6, which results in the X-linked mental retardation disorder Börjeson-Forssman-Lehmann syndrome, is also present in about 38% of adult T-cell acute lymphoblastic leukemias and 3% of adult acute myeloid leukemias. However, it remains to be determined exactly how PHF6 acts *in vivo* and what functions of PHF6 may be associated with its putative tumor suppressor function. Here, we demonstrate that PHF6 is a nucleolus, ribosomal RNA promoter-associated protein. PHF6 directly interacts with upstream binding factor (UBF) through its PHD1 domain and suppresses ribosomal RNA (rRNA) transcription by affecting the protein level of UBF. Knockdown of PHF6 impairs cell proliferation and arrests cells at G_2/M phase, which is accompanied by an increased level of phosphorylated H2AX, indicating that PHF6 deficiency leads to the accumulation of DNA damage in the cell. We found that increased DNA damage occurs at the ribosomal DNA (rDNA) locus in PHF6-deficient cells. This effect could be reversed by knocking down UBF or overexpressing RNASE1, which removes RNA-DNA hybrids, suggesting that there is a functional link between rRNA synthesis and genomic stability at the rDNA locus. Together, these results reveal that the key function of PHF6 is involved in regulating rRNA synthesis, which may contribute to its roles in cell cycle control, genomic maintenance, and tumor suppression.

PHF6, which encodes a protein with PHD-type zinc finger domains, was first identified as a gene associated with Börjeson-Forssman-Lehmann syndrome (BFLS),[2] an X-linked mental retardation disorder (1). BFLS patients have distinctive facial features and suffer from mental retardation, obesity, seizures, gynecomastia, and hypogonadism (2, 3). To date, loss of function mutations and disruptions of the *PHF6* gene are the only factors known to cause BFLS. Because the *PHF6* gene is located on the X chromosome, BFLS patients are almost exclusively male. Interestingly, somatic mutations and deletions of PHF6 have been presented in 16 and 38% of pediatric and adult T-ALL samples, respectively (4). The *PHF6* mutations have also been associated with certain T-ALL subtypes, such as leukemias driven by aberrant expression of the homeobox transcription factor oncogenes *TLX1* and *TLX3* (4). Indeed, a clinical study has described a child with BFLS that developed T-ALL (5). These data suggest that PHF6 mutations may represent a novel genetic alteration that contributes to the development of T-ALL. Moreover, recurrent mutations of PHF6 have been found in about 3% of adult patients with acute myeloid leukemias (6), indicating that PHF6 probably functions as a tumor suppressor. However, despite the devastating effects of mutation of the *PHF6* gene, little is known about the cellular function of PHF6.

PHF6 protein contains two conserved PHD domains. Many PHD-containing proteins, such as PHF8 and ING2, are involved in transcriptional regulation by recognizing different methylated histone tails and modulating chromatin structures (7–12). Unlike typical Cys_4-His-Cys_3 PHD-type zinc fingers, PHF6 contains two imperfect PHD domains (PHD1, residues 82–131: Cys_4-His-Cys-His; PHD2, residues 280–329: Cys_4-His-Cys-His), suggesting that the PHD domains of PHF6 may have functions that differ from other PHD domains.

In this study, we focused on elucidating the cellular functions of PHF6. We found that PHF6 localizes to the nucleolus, directly interacts with upstream binding factor (UBF), and suppresses ribosomal RNA (rRNA) transcription by affecting the protein level of UBF. Moreover, PHF6 deficiency leads to impaired cell proliferation, cell cycle arrest at G_2/M phase, and increased DNA damage at the rDNA locus. Taken together, these results suggest that the tumor suppressor function of PHF6 may be associated with its regulatory role in rRNA synthesis, which contributes to genome maintenance.

* This work was supported, in whole or in part, by National Institutes of Health Grants CA089239, CA092312, and CA100109 (to J. C.).
[1] Recipient of an Era of Hope Scholar award from the Department of Defense (Grant W81XWH-05-1-0470) and a member of M. D. Anderson Cancer Center (National Institutes of Health Grant CA016672). To whom correspondence should be addressed: Dept. of Experimental Radiation Oncology, Unit 66, University of Texas MD Anderson Cancer Center, 1515 Holcombe Blvd., Rm. Y3.6006, Houston, TX 77030. Tel.: 713-792-4863; Fax: 713-794-5369; E-mail: jchen8@mdanderson.org.
[2] The abbreviations used are: BFLS, Börjeson-Forssman-Lehmann syndrome; PHD, plant homeodomain; UBF, upstream binding factor; FUrd, fluorouridine; SFB, streptavidin binding peptide; γ-H2AX, phosphorylated H2AX; rRNA, ribosomal RNA; rDNA, ribosomal DNA.

EXPERIMENTAL PROCEDURES

Cell Culture, RNA Interference, and Antibodies—293T and HeLa cells were maintained in RPMI 1640 medium supplemented with 10% fetal bovine serum and 1% penicillin/streptomycin at 37 °C in a humidified incubator with 5% CO_2 (v/v).

shRNAs against human PHF6 or UBF were purchased from Open Biosystems. The sequence of PHF6 shRNA is CCGGCAGAATTTGGAGACTTTGATACTCGAGTATCAAAGTCTCCAAATTCTGTTTTT. The sequence of UBF shRNA is CCGGGCCTATCACAAGAAGTGTGATCTCGAGATCACACTTCTTGTGATAGGCTTTTT.

The primary antibodies used in this study were as follows: anti-Myc antibody (sc-40, Santa Cruz Biotechnology, Inc. (Santa Cruz, CA)); anti-FLAG antibody (F1804, Sigma-Aldrich); monoclonal anti-GST (sc-138, Santa Cruz Biotechnology, Inc.); anti-UBF antibody (sc-13125, Santa Cruz Biotechnology, Inc.); anti-MBP antibody (05-499, Millipore); anti-BrdU antibody (B2531, Sigma-Aldrich); and anti-fibrillarin antibody (ab5821, Abcam). Anti-PHF6 antibodies were raised by immunizing rabbits with GST-PHF6 fusion proteins containing residues 150–325 of human PHF6. Antisera were affinity-purified using the AminoLink Plus immobilization and purification kit (13).

Cell Proliferation and Cell Cycle Analysis—PHF6-deficient, reconstituted, or control cells were seeded at low density (100,000 cells/10-cm plate). Cell numbers were quantified every day or every other day by digesting cells into suspension using trypsin/EDTA and resuspending in a given volume of fresh medium. The data presented represent the mean of all measured points ± S.E. ($n = 5$).

FACS for determination of cell cycle distribution was performed using propidium iodide staining. Briefly, 1×10^6 cells were harvested, washed twice with PBS, resuspended in 300 μl of PBS, and then fixed with the addition of 700 μl of 100% ethanol. After storage at −20 °C overnight, fixed cells were washed and incubated in sodium citrate buffer containing RNase A for 30 min and then stained with propidium idodide for 30 min. Cells were then run on a FACScan system, and cell cycle analysis was performed.

Co-precipitation and Western Blotting—Cells were lysed with NTEN buffer (20 mM Tris-HCl, pH 8.0, 100 mM NaCl, 1 mM EDTA, 0.5% Nonidet P-40) containing protease inhibitors on ice for 20 min. The soluble fractions were collected after centrifugation and incubated either with protein A-agarose beads coupled with anti-PHF6 or anti-UBF antibodies or with S-protein-agarose beads (Novagen) for 3 h at 4 °C. The beads were then washed three times and boiled in 2× SDS loading buffer. Samples were resolved on SDS-PAGE and transferred to PVDF membrane, and immunoblotting was carried out with antibodies as indicated.

Immunofluorescence Staining—Cells were normally fixed in 3% paraformaldehyde for 10 min and then permeabilized in 0.5% Triton X-100-containing solution for 5 min on ice. For immunostaining using PHF6 antibody, cells were fixed in acetone/methanol mixture (1:1) at −20 °C for 12 min. Cells were incubated with primary antibodies diluted in 5% goat serum at 37 °C for 30 min. After washing with PBS twice, cells were incubated with either FITC- or rhodamine-conjugated secondary antibodies for 30 min at 37 °C. Nuclei were counterstained with DAPI and then mounted onto glass slides with anti-fade solution. Images were taken with a Nikon ECLIPSE E800 fluorescence microscope with a Nikon Plan Fluor ×60 oil objective lens (numerical aperture 1.30) at room temperature. Cells were photographed using a SPOT camera (Diagnostic Instruments, Inc.) and analyzed using Photoshop software (Adobe).

GST Pull-down Assay—GST fusion proteins were expressed in *Escherichia coli* and purified as described previously (14). GST fusion proteins were immobilized on glutathione-Sepharose 4B beads and incubated with lysates prepared from cells transiently transfected with plasmids encoding the indicated proteins. The samples were subjected to SDS-PAGE and analyzed by Western blotting.

Chromatin Immunoprecipitation (ChIP) Assay—The ChIP assay was performed with a ChIP assay kit (catalog no. 17-295, Millipore) following the manufacturer's recommendations. Briefly, chromatin from cross-linked HeLa cells was sheared using the Covaris S2 system to a size range of 100–400 bp. Immunoprecipitation was conducted with either a specific antibody (FLAG antibody or homemade phospho-H2AX antibody), or mock IgG-conjugated Protein A (rabbit)- or G (mouse)-Sepharose beads. The reverse of cross-linking was performed at 70 °C overnight. After RNase A and Proteinase K treatment, sample was deproteinized with UltraPure phenol/chloroform/isoamyl alcohol (Invitrogen) and further purified with the Qiaquick PCR purification kit (Qiagen). Purified immuno-enriched samples were amplified by quantitative PCR and calculated as the ratio of immunoprecipitated rDNA *versus* rDNA in the input chromatin. Primers were as follows: Primer A, forward (5′-AGGTGTCCGTGTCCGTGT-3′) and reverse (5′-GGACAGCGTGTCAGCAATAA-3′); Primer B, forward (5′-TCCTGCTCAGTACGAGAG-3′) and reverse (5′-GACAAACCCTTGTGTCGAGG-3′); primer for β-actin promoter, forward (5′-GCCCAGCACCCCAAGGCGGCCA-3′) and reverse (5′GTCTCGGCGGTGGTGGCGCGTC-3′).

The specificity of phospho-H2AX antibody for the ChIP assay was confirmed in U2OS-DR-GFP cells, which contain a single complete copy of the integrated hypoxanthine-guanine phosphoribosyltransferase-DR-GFP (13). U2OS-DR-GFP cells (1.5×10^5 cells/well) were seeded in 6-well plates and, the following morning, transfected with 1 μg of pCBA-I-SceI. Cells were harvested 18 h after transfection for ChIP analysis using phospho-H2AX antibody.

RNA Analysis—We isolated RNA with TRIzol reagent (Invitrogen) and transcribed the RNA into cDNAs using random primers. To monitor the level of pre-rRNA, we amplified cDNA by quantitative RT-PCR using primers that amplify human rDNA sequences (forward, 5′-CCGCGCTCTACCTTACCTAC-3′; reverse, 5′-GAGCGACCAAAGGAACCATA-3′). We measured the PHF6 mRNA level using the following primers: forward, 5′-TTGGTGGATTTTCTATTGAAGATGT-3′; reverse, 5′-TTGATGTTGTTGTGAGCTGGACTGT-3′). For normalization, we measured β-actin mRNA level using the forward primer 5′-CGTCACCAACTGGGACGACA-3′ and the reverse primer 5′-CTTCTCGCGGTTGGCCTTGG-3′.

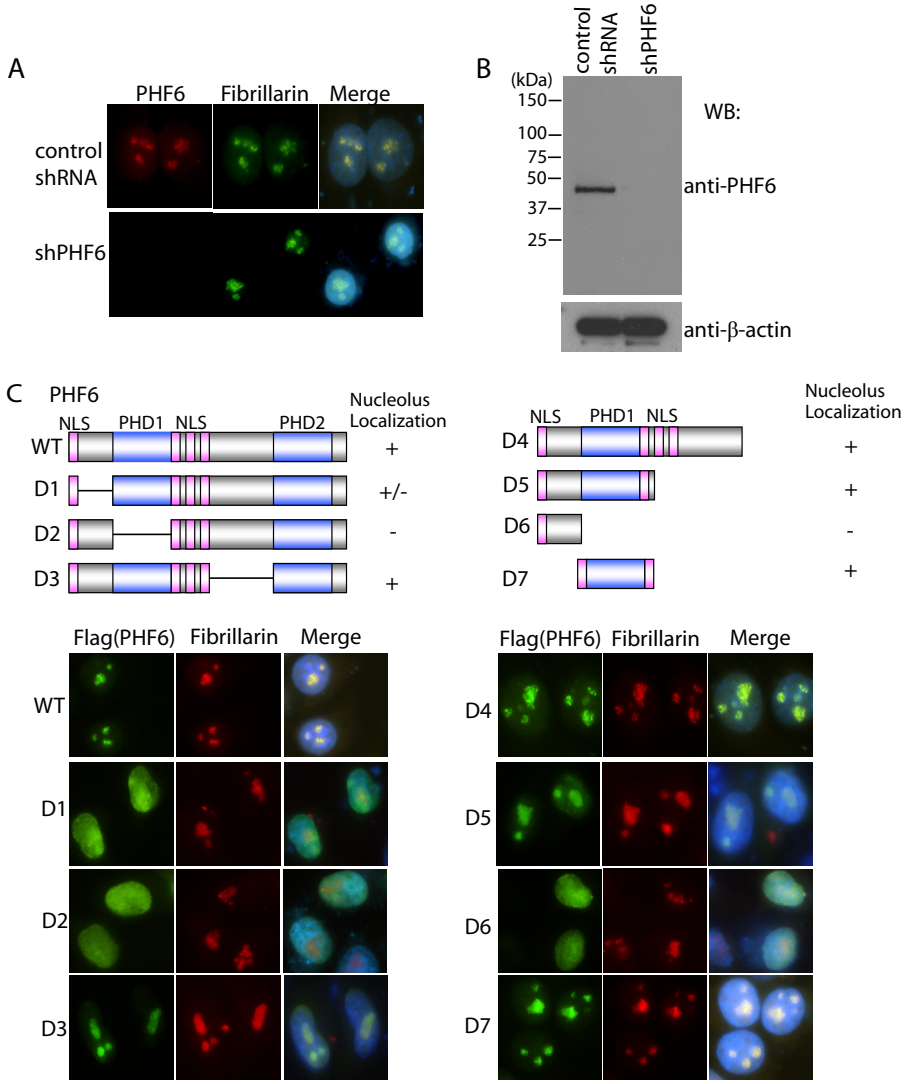

FIGURE 1. **PHF6 localizes in nucleolus.** *A*, PHF6 localized in nucleolus. HeLa cells transfected with control shRNA or PHF6-specific shRNA were fixed, and immunostaining was carried out using the indicated antibodies. *B*, validation of the specificity of PHF6 antibody and shRNA-mediated PHF6 knockdown efficiency. Stable PHF6 knockdown cells or control HeLa cells were lysed and subjected to Western blotting (*WB*) using anti-PHF6 antibody. *C*, PHF6 localization to nucleolus requires its PHD1 domain. HeLa cells were transfected with plasmids encoding SFB-tagged wild type or deletion mutants of PHF6. Cells were fixed and immunostained with anti-FLAG and anti-fibrillarin antibodies. A schematic diagram of PHF6 shows the PHD1 domain, PHD2 domain, and nuclear localization signal (*NLS*).

Fluorouridine (FUrd) Staining and Incorporation—Cells were labeled with 5-fluorouridine for 10 min. Cells were then fixed, and 5-fluorouridine incorporation was revealed by the use of specific fluorescein isothiocyanate-conjugated antibodies. The quantification of FUrd incorporation was performed as described previously (15).

Tandem Affinity Purification of PHF6-associated Protein Complex—293T cells stably expressing streptavidin binding peptide (SFB)-PHF6 were lysed with NETN buffer (20 mM Tris·HCl, pH 8, 100 mM NaCl, 1 mM EDTA, 0.5% Nonidet P-40) on ice for 20 min. Cell lysates were treated in the presence or absence of micrococcal nuclease (Roche Applied Science) for 5 min at 37 °C, followed by centrifugation at 13,000 × *g* for 20 min at 4 °C. Supernatant was incubated with streptavidin beads for 2 h at 4 °C. Bound complex was eluted with 2 mg/ml biotin diluted in NETN. Supernatant was further incubated with S protein-conjugated agarose beads for 2 h at 4 °C. Beads were washed three times with NETN buffer, and proteins bound to the beads were eluted by boiling with SDS sample buffer. Proteins were resolved by SDS-PAGE and submitted for mass spectrometry analysis for protein identification by the Taplin biological mass spectrometry facility (Harvard University).

RESULTS

PHF6 Localizes in the Nucleolus via Its PHD1 Domain—To explore the subcellular localization of endogenous PHF6, we generated anti-PHF6 antibody and used it for immunofluorescent staining. We found that endogenous PHF6 localized in the nucleolus (Fig. 1*A*) and co-localized with a nucleolus marker, fibrillarin (Fig. 1*A*), which is rRNA 2′-*O*-methyltransferase and normally localizes in the nucleolus (16, 17). This staining was absent in PHF6 knockdown cells (Fig. 1*A*), indicating that our antibody specifically recognizes endogenous PHF6. The speci-

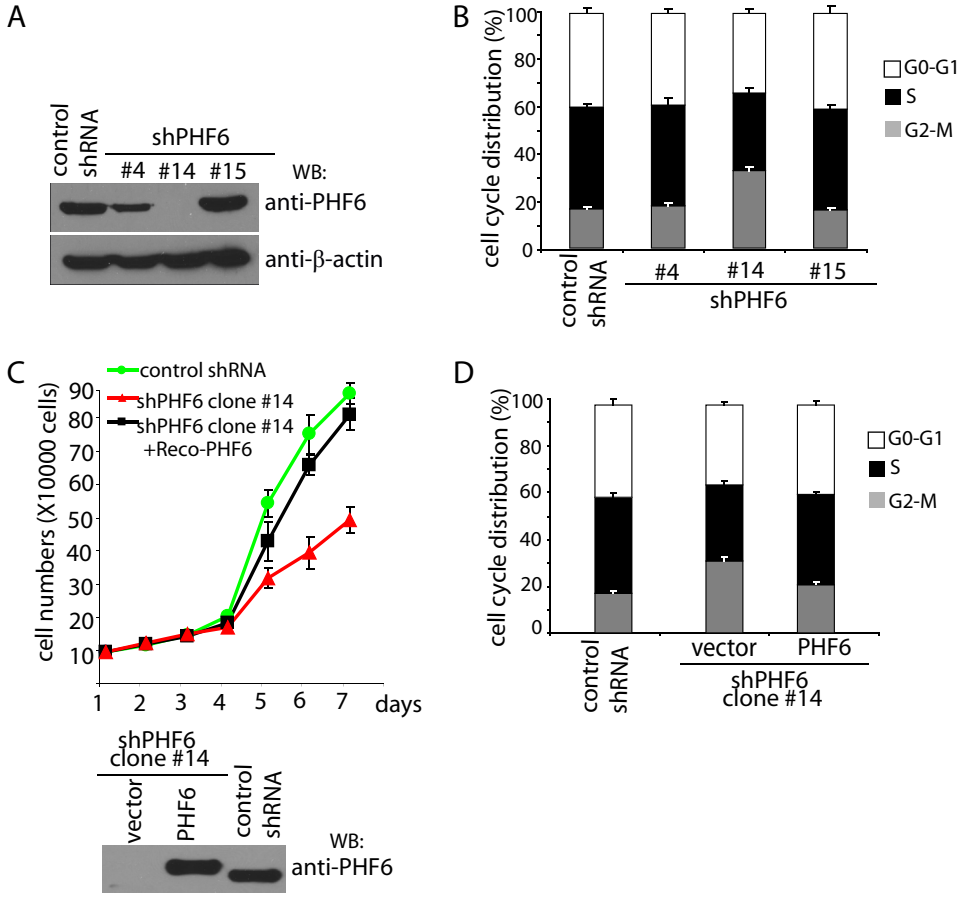

FIGURE 2. **PHF6 knockdown impairs cell proliferation and arrests cells at G_2/M phase.** *A*, establishment of PHF6 stable knockdown cell lines. HeLa cells were transfected with control shRNA or plko.1-PHF6 and cultured in medium containing puromycin. The clones were selected, and down-regulation of PHF6 expression in these clones was examined by Western blotting (*WB*) using anti-PHF6 antibodies. *B*, knockdown of PHF6 arrests cells in G_2/M phase. PHF6 depletion or control cells were collected and analyzed by flow cytometry to assess cell cycle distribution by propidium iodide staining. *C*, knockdown of PHF6 impairs cell proliferation. Control transfected cells, PHF6-depleted cells (clone 14), or PHF6-depleted cells reconstituted with PHF6 expression were seeded at low density, and cell proliferation was measured by determining the cell numbers every day. *Error bars*, S.D. from at least three independent experiments. PHF6 expression in these cells was confirmed by Western blotting as indicated. *D*, reconstitution of wild type PHF6 rescued cell cycle arrest observed in PHF6-depleted cells. HeLa cells with PHF6 depletion were infected with retrovirus expressing FLAG-tagged PHF6. Cells were then collected and analyzed by flow cytometry to assess cell cycle distribution.

ficity of our anti-PHF6 antibody was also confirmed by Western blotting (Fig. 1*B*).

To define the region(s) of PHF6 required for its nucleolus localization, triple-tagged (S-protein-, FLAG-, and SFB-tagged) wild type PHF6 and a series of PHF6 deletion mutants were transfected into HeLa cells (Fig. 1*C*). Results indicated that deletion of the N terminus or the PHD1 domain of PHF6 led to a dramatic decrease in PHF6 nucleolus localization (Fig. 1*C*). In addition, we found that the PHD1 domain alone, not the N terminus, was sufficient for its nucleolus localization (Fig. 1*C*). Together, these data suggest that PHF6 is a nucleolus protein, and its nucleolus localization mainly depends on its PHD1 domain.

Knockdown of PHF6 Impairs Cell Proliferation and Arrests Cells in G_2/M Phase—To gain insight into the cellular functions of PHF6, we generated PHF6 stable knockdown cells and control cells using PHF6-targeting and non-targeting shRNAs, respectively, in HeLa cells. Three stable cell lines with different levels of PHF6 knockdown were selected for further analysis (Fig. 2*A*).

When we examined cell cycle distribution, we found that cells with a nearly complete depletion of PHF6 expression (clone 14) had a higher fraction of G_2/M phase cells than those observed in control cells (Fig. 2*B*), suggesting that the absence of PHF6 may affect cell cycle transitions, which could reduce cell proliferation. Indeed, complete knockdown of PHF6 dramatically inhibited cell proliferation when compared with those of control cells (Fig. 2*C*). To confirm that the observed cell proliferation defect was indeed a consequence of PHF6 deficiency, we reconstituted PHF6 expression in these PHF6 knockdown cells using a retroviral PHF6 expression vector (Fig. 2*C*). Restoring PHF6 expression largely rescued the cell proliferation defect in these cells (Fig. 2*C*). Moreover, it also restored normal cell cycle distribution (Fig. 2*D*). These results indicate that PHF6 is required for normal cell cycle progression.

PHF6 Binds to rDNA Promoter and Suppresses rRNA Synthesis—The nucleolus localization of PHF6 indicates that PHF6 may play a role in nucleolar chromatin-based processes. As a matter of fact, ChIP assays confirmed that PHF6 associates with the rDNA promoter (Fig. 3*A*), suggesting that PHF6 may be involved in rDNA transcriptional regulation. To test this possibility, we measured pre-rRNA synthesis in control cells and in cells with shRNA-mediated depletion of PHF6. Reverse transcription-polymerase chain reaction (RT-PCR) analysis

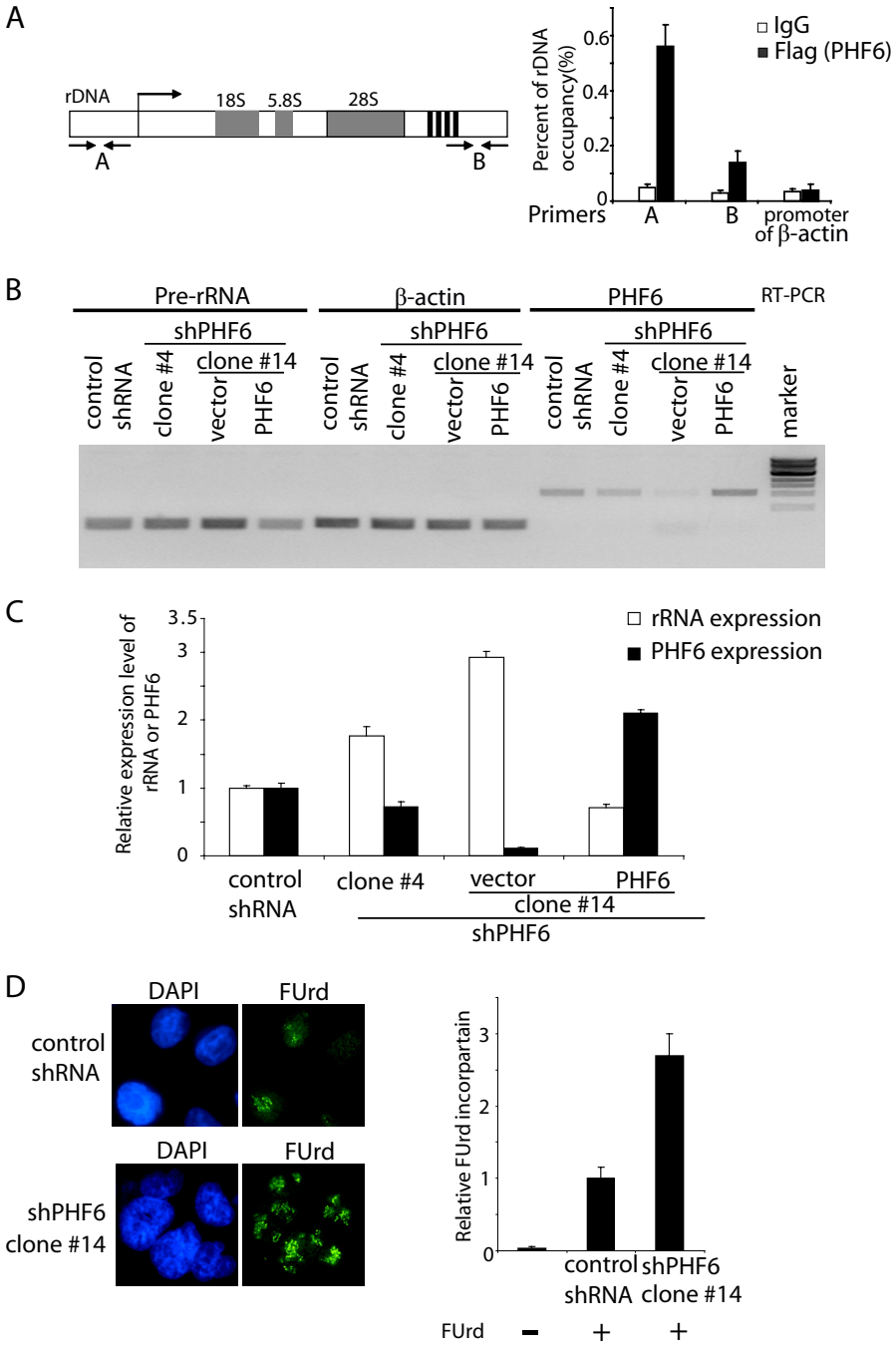

FIGURE 3. **PHF6 binds to rDNA promoter and suppresses rRNA synthesis.** *A*, PHF6 binds to rDNA promoter. HeLa cells stably expressing FLAG-tagged PHF6 were generated. ChIP assays were performed by using control IgG or anti-FLAG antibody. Purified immuno-enriched samples were analyzed by real-time PCR using primer pairs that amplify the indicated regions of human rDNA. *Error bars*, S.D. from at least three independent experiments. *B*, PHF6 suppresses rRNA synthesis. Total RNA was extracted from the indicated cells, and RT-PCR was performed using the indicated sequence-specific PCRs. *C*, relative levels of pre-rRNA were determined by real-time quantitative PCR in the indicated cells. Values are obtained by normalizing the rRNA levels with β-actin mRNA levels. *Error bars*, S.D. ($n = 3$). *D*, ribosomal RNA synthesis was assessed by FUrd (10 μg/ml) incorporation in HeLa cells. Cells were labeled with fluorouridine for 10 min and then fixed and immunostained using anti-BrdU antibody. The FUrd incorporation was quantitated. *Error bars*, S.D. ($n = 3$).

revealed that rDNA transcription was significantly increased after complete knockdown of PHF6 (clone 14) and moderately increased after partial knockdown of PHF6 (clone 4) (Fig. 3*B*), suggesting that PHF6 negatively regulates rRNA synthesis. As a control, we showed that reconstitution of PHF6 expression in PHF6 knockdown cells largely reversed the increase in pre-rRNA level (Fig. 3*B*). The rDNA transcriptional activity was further confirmed by real-time PCR using primer pairs that amplify the human pre-rDNA (Fig. 3*C*).

To further establish the relationship between PHF6 and rRNA transcriptional regulation, rRNA synthesis was assessed by a FUrd incorporation assay as described previously (15). We observed a pronounced increase in FUrd incorporation in PHF6-depleted cells compared with those in control cells (Fig.

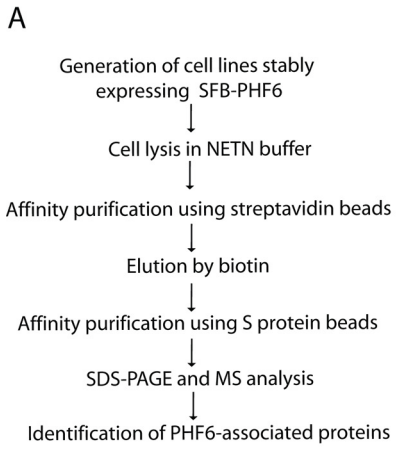

B

PHF6 and its associated proteins	Number of peptides identified by M.S.
PHF6	31
UBF	19
RPS3	17
CHD1	12
HAT1	6
CHD2	5
ILF2	4
DDB1	3
VPRBP	3

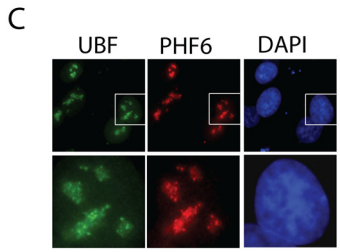

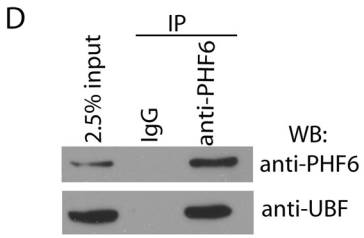

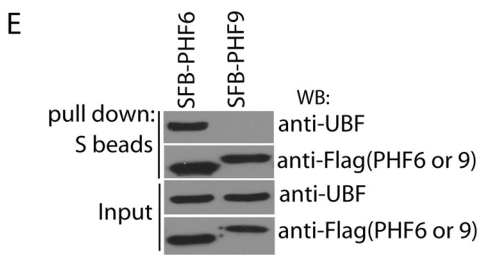

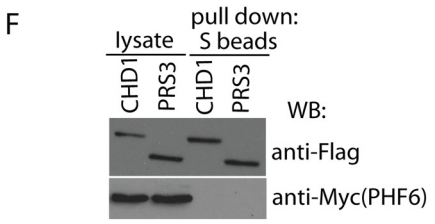

FIGURE 4. **PHF6 interacts with UBF.** *A*, schematic representation of SFB-PHF6 purification strategy. *B*, list of PHF6-associated proteins identified by mass spectrometric analysis. PHF6-containing complexes were isolated from 293T cells and subjected to mass spectrometry analysis. *C*, endogenous PHF6 and UBF co-localize in the nucleolus. HeLa cells were fixed and immunostained with anti-PHF6 and anti-UBF antibodies. The cell indicated was enlarged in the *lower panel*. *D*, immunoprecipitation (*IP*) reactions were performed using Jurkat cell lysates, which were then subjected to immunoblotting (*WB*) using the indicated antibodies. *E*, 293T cells were transfected with plasmids encoding SFB-tagged PHF6 or control PHF9. Precipitation reactions were carried out using S-protein beads and then subjected to immunoblotting using the indicated antibodies. *F*, CHD1 and RPS3 failed to interact with PHF6. 293T cells were transfected with constructs encoding SFB-tagged CHD1 or RPS3 together with Myc-tagged PHF6. 24 h later, cells were collected. Precipitation reactions were performed using S-protein beads and then subjected to immunoblotting using antibodies as indicated.

3*D*), further confirming that PHF6 negatively regulates rRNA synthesis.

PHF6 Interacts with UBF—Next, we wanted to understand exactly how PHF6 acts in regulating rRNA synthesis. We carried out tandem affinity purification using lysates prepared from 293T cells stably expressing SFB-tagged PHF6 (Fig. 4*A*). Mass spectrometry analysis revealed that UBF, a transcription factor required for the expression of ribosomal RNAs, is a major PHF6-associated protein (Fig. 4*B*).

Endogenous PHF6 and UBF co-localized in distinct foci within the nucleolus, suggesting that these two proteins may work in concert (Fig. 4*C*). Co-precipitation assays confirm the interaction between overexpressed proteins and endogenous proteins, respectively (Fig. 4, *D* and *E*). We also checked some other candidate proteins from PHF6 purification results, such as CHD1 and RPS3. However, none of them interact with PHF6 *in vivo* (Fig. 4*F*).

UBF Recruits PHF6 to rDNA Promoter—To reveal which domain or domains of PHF6 are required for its association with UBF, SFB-tagged wild type PHF6 and a series of PHF6 deletion mutants were subjected to co-precipitation experiments (Fig. 5*A*). Results indicated that deletion of the PHD1 domain of PHF6 abolished the PHF6-UBF interaction, whereas deletion of the PHD2 domain of PHF6 also reduced PHF6-UBF interaction (Fig. 5*A*), suggesting that the PHD domains of PHF6 are responsible for its binding to UBF, with the PHD1 domain of PHF6 as the critical binding site for UBF.

Because the PHD1 domain of PHF6 is required for both nucleolus localization and UBF binding (Figs. 1*B* and 5*A*), we speculated that UBF might recruit PHF6 to the rDNA promoter. Indeed, the ChIP assay showed that knockdown of UBF decreased the binding of PHF6 to the rDNA promoter (Fig. 5*B*), suggesting that UBF is at least partially responsible for recruiting PHF6 to the rDNA locus.

We further explored whether any missense mutations of PHF6 within the PHD1 domain identified in patients would affect the PHF6-UBF binding. We used two mutants, the C45Y and the C99F mutants of PHF6 (Fig. 5*C*). Interestingly, both of

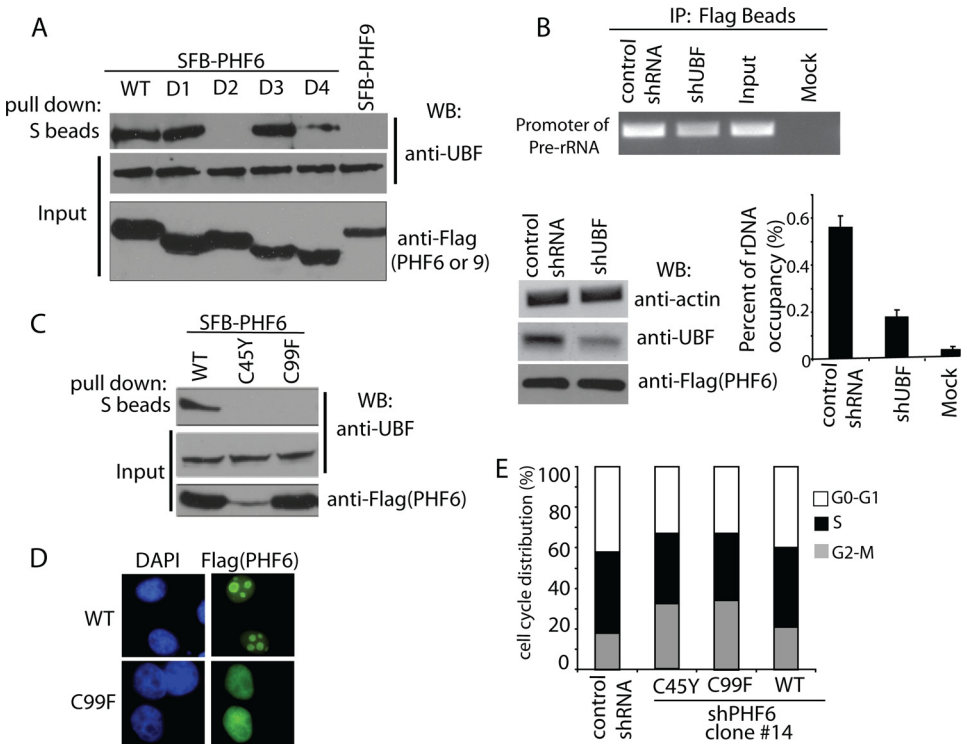

FIGURE 5. **UBF recruits PHF6 to rDNA promoter.** *A*, mapping of the corresponding regions required for PHF6-UBF interaction. Precipitation reactions were performed using S-protein beads, which were then subjected to immunoblotting (*WB*) using antibodies as indicated. Schematic diagrams of wild type and deletion mutants of PHF6 are shown in Fig. 1*C*. *B*, UBF recruits PHF6 to the rDNA promoter. ChIP assays were performed in HeLa cells stably expressing PHF6 with or without infection with viral particles expressing UBF shRNAs. Purified immuno-enriched samples and input genomic DNA samples were used for sequence-specific PCRs. UBF knockdown was confirmed by Western blotting as indicated. ChIP assays were also analyzed by real-time PCR and quantified. *IP*, immunoprecipitation. *Error bars*, S.D. from at least three independent experiments. *C*, C99F mutant of PHF6 failed to interact with UBF. 293T cells were transfected with constructs encoding SFB-tagged wild type PHF6, C45Y, or C99F mutant of PHF6. 24 h later, cells were collected. Precipitation reactions were performed using S-protein beads and then subjected to immunoblotting using antibodies as indicated. *D*, C99F mutant failed to localize in the nucleolus. HeLa cells were transfected with plasmids encoding SFB-tagged wild type or C99F mutants of PHF6. Cells were fixed and immunostained with anti-FLAG antibody. *E*, reconstitution of C45Y or C99F mutant failed to rescue cell cycle arrest observed in PHF6-depleted cells. HeLa cells with the PHF6 depletion were infected with retrovirus expressing FLAG-tagged wild type or the C45Y or C99F mutant of PHF6. Cells were collected and analyzed by flow cytometry to assess cell cycle distribution.

these mutants abolished the PHF6-UBF binding (Fig. 5*C*), however probably through different mechanisms. The C45Y mutant was not expressed well in the cell (Fig. 5*C*), indicating that this mutation may affect protein stability. The C99F mutant was expressed to a level similar to that of wild type PHF6; however, this mutant is defective in UBF binding (Fig. 5*C*), suggesting that this residue, which locates at the center of the PHD1 domain, is required for PHF6-UBF interaction. In agreement with our hypothesis that UBF recruits PHF6 to nucleolus, the C99F mutant of PHF6 failed to localize to the nucleolus (Fig. 5*D*).

Next we assessed whether any of these two mutants could rescue the G_2/M arrest in PHF6-depleted cells. PHF6 knockdown cells were reconstituted with wild type or the C45Y or C99F mutant of PHF6. As expected, only wild type PHF6, and neither of the PHF6 mutants, could restore the normal cell cycle distribution (Fig. 5*E*).

PHF6 Deficiency Leads to Increased DNA Damage at the rDNA Locus—It was puzzling why increased rRNA synthesis would associate with reduced cell proliferation and G_2/M arrest in PHF6-depleted cells. One clue is that we and others have observed increased phosphorylated H2AX (γ-H2AX) in PHF6-deficient cells (Fig. 6*A*) (4). We speculated that deregulation of rRNA synthesis in the absence of PHF6 might result in DNA damage and thus account for G_2/M arrest and reduced cell proliferation. If this is the case, we should observe DNA damage specifically occurring at the rDNA locus. To test this possibility, a ChIP assay was performed using phospho-H2AX antibody. First, we determined whether the phospho-H2AX antibody we have works for a ChIP assay. Double strand breaks were generated by I-SceI at the GFP locus in U2OS-DR-GFP cells, which are routinely used to measure I-SceI-induced DNA damage repair (Fig. 6*B*). ChIP assays were performed using phospho-H2AX antibody. As shown in Fig. 6*B*, phosphorylated H2AX antibody specifically immunoprecipitated DNA around the GFP site following the introduction of double strand breaks by I-SceI. However, we did not detect any signal in mock-transfected cells or at the β-actin promoter (Fig. 6*B*), suggesting that our phospho-H2AX antibody works for the ChIP assay. Next, we performed ChIP assays at the rDNA locus using this phospho-H2AX antibody. We observed increased DNA damage at the rDNA locus specifically in PHF6-deficient cells but not in control cells or at the β-actin promoter region (Fig. 6, *C* and *D*). In PHF6-deficient cells reconstituted with PHF6 expression, the occupancy of phospho-H2AX on the rDNA locus was clearly decreased, suggesting that depletion of PHF6 specifically results in DNA damage at the rDNA locus (Fig. 6, *C* and *D*).

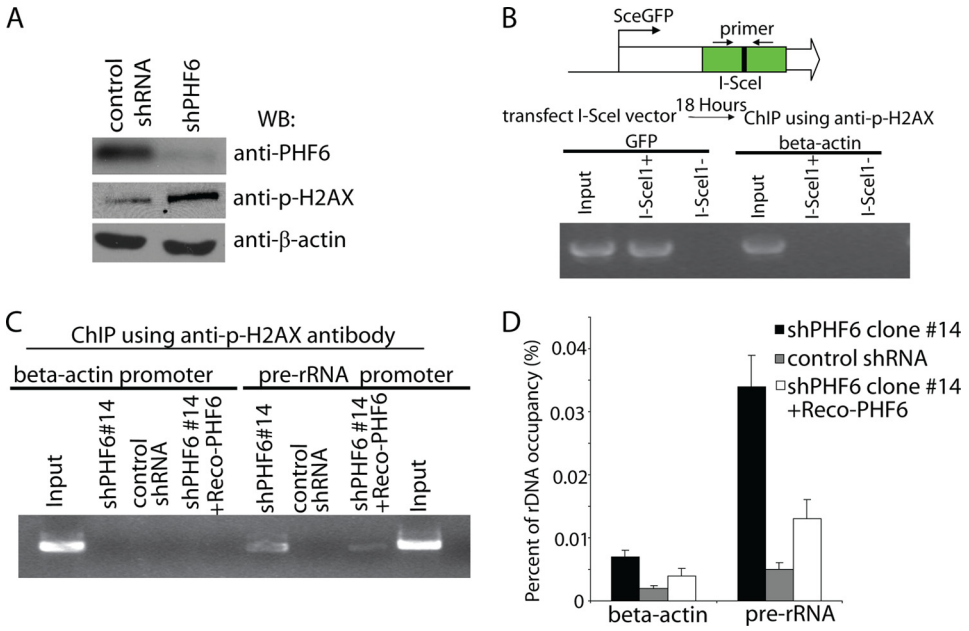

FIGURE 6. **PHF6 deficiency leads to increased DNA damage at the rDNA locus.** *A*, PHF6 deficiency induced DNA damage. PHF6-depleted HeLa cells or control cells were lysed and subjected to Western blotting (*WB*) using the indicated antibodies. *B*, U2OS-DR-GFP cells were transfected with 1 μg of pCBA-I-SceI plasmid. 18 h later, cells were collected, and cell lysates were subjected to ChIP using γ-H2AX antibody. Purified immuno-enriched samples and genomic DNA samples (as input) were used for sequence-specific PCRs. *C*, PHF6 deficiency induced DNA damage at the rDNA locus. PHF6 depletion or control cells or reconstitution cells were collected and subjected to ChIP by using γ-H2AX antibody. Purified immuno-enriched samples were analyzed by sequence-specific PCRs. The PCR primers target to the rDNA region or β-actin region. *D*, purified immuno-enriched samples from *C* were analyzed by real-time PCR using primer pairs that amplify the region of human rDNA. *Error bars*, S.D. from at least three independent experiments.

PHF6 Deficiency Leads to Increased DNA Damage at the rDNA Locus by Increasing UBF Protein Level and RNA-DNA Hybrids—Next, we explored how PHF6 may suppress rRNA synthesis. PHF6 strongly interacts with UBF *in vivo* and *in vitro*. UBF contains a transactivation domain and several HMG domains that are required for DNA binding and the activation of rDNA transcription. Thus, it is possible that PHF6 may suppress rDNA transcription by inhibiting UBF activity. Interestingly, we found that in PHF6-deficient cells, the protein level of UBF was higher than that in control cells (Fig. 7*A*). Moreover, reconstitution of PHF6 in PHF-deficient cells resulted in normal UBF expression in these cells (Fig. 7*A*), suggesting that PHF6 may suppress rDNA transcription by regulating UBF expression level.

If DNA damage occurring at the rDNA locus was induced by higher expression of UBF in PHF6-depleted cells, reducing UBF expression should reverse this effect. To test this possibility, we generated UBF and PHF6 double knock-down cells, which could reduce the UBF expression to a level close to that in control cells (Fig. 7*B*). As shown in Fig. 7*C*, reducing UBF expression in PHF6 knockdown cells diminished DNA damage at rDNA.

We further confirmed these phenotypes of PHF6 knockdown in a different cell line. We picked Jurkat cells, because these cells express wild type PHF6. As shown in Fig. 7, *D* and *E*, knockdown of PHF6 in Jurkat cells also resulted in increasing UBF protein level, H2AX phosphorylation, and G_2/M accumulation, suggesting that the phenotypes we described in HeLa knockdown cells are also reproducible in other cell lines.

Knocking down UBF expression not only diminished DNA damage at rDNA (Fig. 7*C*); it also largely rescued cell cycle arrest and cell proliferation defect in PHF6-depleted cells (Fig. 7, *F* and *G*). We reason that the underlying mechanism may be the formation of a RNA-DNA hybrid, because it has been reported recently that abnormal RNA synthesis would result in DNA double strand breaks and instability at the ribosomal DNA region through the formation of RNA-DNA hybrids (18, 19). To explore whether DNA damage at the rDNA locus induced by PHF6 depletion would result from the formation of RNA-DNA hybrids, we overexpressed RNASE1H in PHF6-depleted cells, which should remove RNA-DNA hybrids *in vivo*. As expected, overexpressing RNASE1 in PHF6-depleted cells diminished DNA damage at the rDNA locus (Fig. 7*H*). These data support our hypothesis that PHF6 regulates UBF expression and rRNA synthesis and helps to maintain normal cell cycle progression and genomic stability (Fig. 7*I*).

DISCUSSION

PHF6 is mutated in T-cell acute lymphoblastic leukemia and, less frequently, in adult acute myeloid leukemia, suggesting that PHF6 may function as a tumor suppressor (4, 6). In this study, we discovered that PHF6 is a nucleolus, rRNA promoter-associated protein that suppresses rRNA transcription. We propose that this function of PHF6 may be linked with its tumor suppressor function.

Characterization of mechanisms that control rRNA synthesis is important for understanding fundamental questions of cancer etiology, because rRNA synthesis is intimately linked to cell growth and frequently up-regulated in many cancers (7, 20). However, loss of PHF6 paradoxically led to higher rRNA synthesis but at the same time impaired cell proliferation and accumulated cells in G_2/M phase. We believe that this discrep-

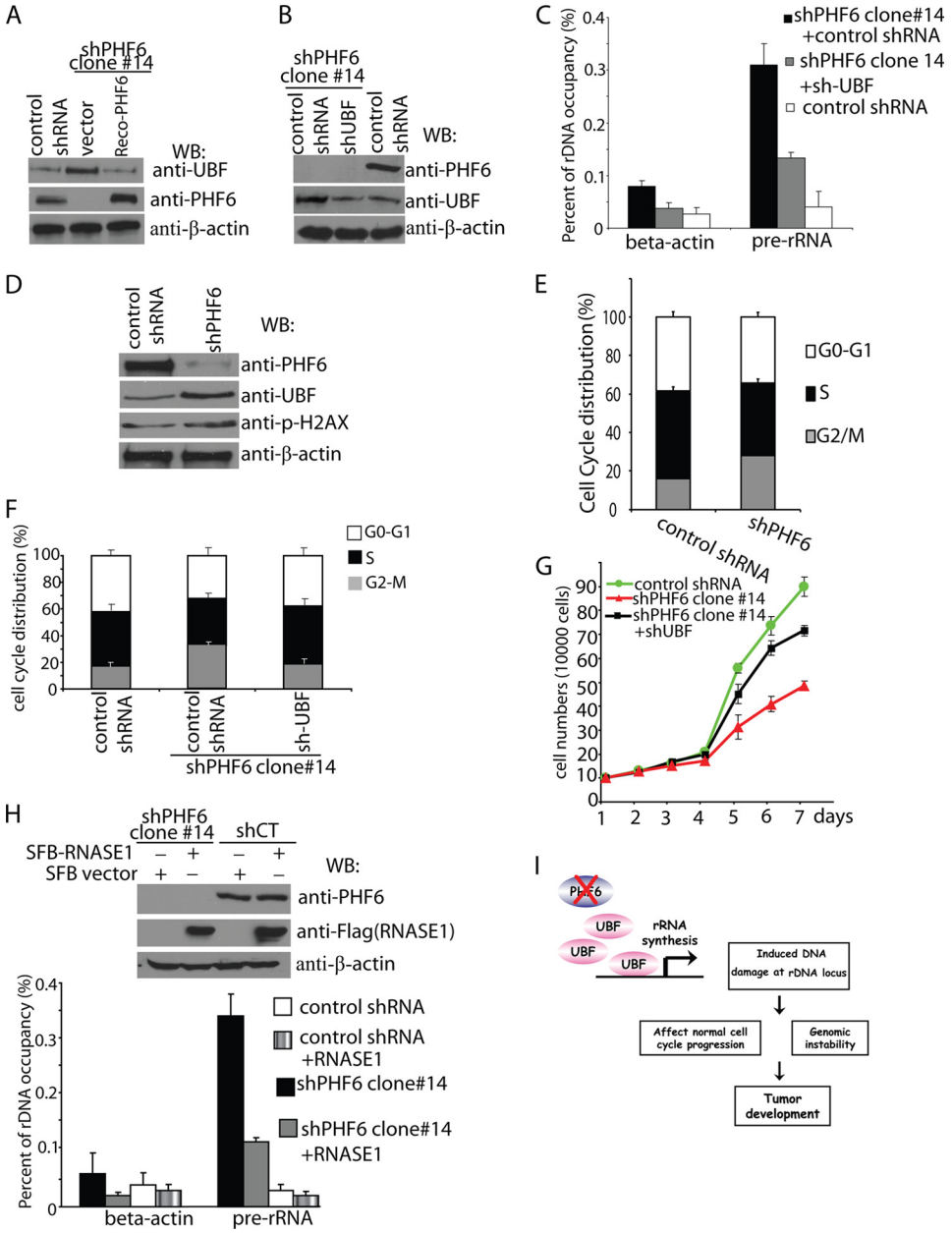

FIGURE 7. **PHF6 deficiency leads to increased DNA damage at the rDNA locus by increasing UBF protein level and RNA-DNA hybrids.** *A*, PHF6 deficiency increased UBF protein level. Lysates prepared from control cells, PHF6-depleted cells, and PHF6-depleted cells reconstituted with PHF6 expression were subjected to immunoblotting (*WB*) using antibodies as indicated. *B*, knockdown of UBF to endogenous level in HeLa cells with PHF6 depletion. HeLa cells with PHF6 depletion were infected with viruses prepared from packaging cells transfected with pGIPZ-shUBF or PGIPZ-shControl. Protein levels of PHF6 and UBF were detected by Western blotting analysis. *C*, knockdown of UBF reduced DNA damage at the rDNA locus in PHF6-depleted cells. PHF6 single knock-down cells or PHF6 and UBF double knock-down cells or control cells were collected and subjected to ChIP using γ-H2AX antibody. Purified immuno-enriched samples were analyzed by real-time PCR using primer pairs that amplify regions of human rDNA or β-actin. *Error bars*, S.D. from at least three independent experiments. *D*, lysates prepared from control Jurkat cells and PHF6-depleted Jurkat cells were subjected to immunoblotting using antibodies as indicated. *E*, PHF6-depleted or control Jurkat cells were collected and analyzed by flow cytometry to assess cell cycle distribution by propidium iodide staining. *Error bars*, S.D. from at least three independent experiments. *F*, knockdown of UBF rescued cell cycle arrest observed in PHF6-depleted cells. HeLa cells with PHF6 depletion were infected with viruses prepared from packaging cells transfected with pGIPZ-shUBF or PGIPZ-shControl. Cells were then collected and analyzed by flow cytometry to assess cell cycle distribution. *G*, knockdown of UBF rescued the cell proliferation defect in PHF6-depleted cells. Control HeLa cells or HeLa cells with PHF6 depletion were infected with infected with viruses prepared from packaging cells transfected with pGIPZ-shUBF or PGIPZ-shControl. Cell proliferation was measured by determining cell number every day. *H*, overexpressing RNase H reduced DNA damage at the rDNA locus in PHF6-depleted cells. HeLa cells with PHF6 depletion or control cells were infected with viruses encoding HA-FLAG-RNase H. 48 h later, cells were collected and subjected to ChIP using γ-H2AX antibody. Purified immuno-enriched samples were analyzed by real-time PCR using primer pairs that amplify regions of human rDNA or β-actin. *Error bars*, S.D. from at least three independent experiments. *I*, proposed model of PHF6 function as a potential tumor suppressor gene.

ancy can be explained by increased DNA damage (as measured by increased phosphorylated H2AX) in PHF6-deficient cells (Fig. 7), which was also reported previously (4). Abnormal up-regulation of rRNA synthesis in the absence of PHF6 may interfere with normal homeostasis regulation of rRNA synthesis and thus result in DNA damage at the rDNA locus, possibly by the formation of RNA-DNA hybrids. This increase in DNA damage at the rDNA locus could then lead to cell cycle arrest and

reduced cell proliferation. We speculate that the increased DNA damage in PHF6-deficient cells may eventually result in genomic instability and contribute to tumorigenesis. If this hypothesis is correct, PHF6 may be classified as a caretaker tumor suppressor, which functions by ensuring proper rRNA synthesis to maintain genomic stability.

This study has a broad impact on our understanding of cancer etiology. Although defects in DNA damage response and DNA repair do contribute to tumorigenesis, mutations of genes involved in these pathways are not frequently observed in human cancers, raising the question as how genomic instability normally arises during tumorigenesis. Our study presented here suggests that deregulation of many cellular pathways, including rRNA synthesis, could be the source of initial genomic instability that promotes tumorigenesis. Many proteins involved in the regulation of various cellular processes could potentially act as tumor suppressors, because in their absence, increased DNA damage and genomic instability may arise, which eventually lead to tumorigenesis.

Acknowledgments—We thank our colleagues in the Chen laboratory for insightful discussion and technical assistance.

REFERENCES

1. Lower, K. M., Turner, G., Kerr, B. A., Mathews, K. D., Shaw, M. A., Gedeon, A. K., Schelley, S., Hoyme, H. E., White, S. M., Delatycki, M. B., Lampe, A. K., Clayton-Smith, J., Stewart, H., van Ravenswaay, C. M., de Vries, B. B., Cox, B., Grompe, M., Ross, S., Thomas, P., Mulley, J. C., and Gécz, J. (2002) Mutations in PHF6 are associated with Börjeson-Forssman-Lehmann syndrome. *Nat. Genet.* **32,** 661–665
2. Visootsak, J., Rosner, B., Dykens, E., Schwartz, C., Hahn, K., White, S. M., Szeftel, R., and Graham, J. M. (2004) Clinical and behavioral features of patients with Borjeson-Forssman-Lehmann syndrome with mutations in PHF6. *J. Pediatr.* **145,** 819–825
3. Turner, G., Lower, K. M., White, S. M., Delatycki, M., Lampe, A. K., Wright, M., Smith, J. C., Kerr, B., Schelley, S., Hoyme, H. E., De Vries, B. B., Kleefstra, T., Grompe, M., Cox, B., Gecz, J., and Partington, M. (2004) The clinical picture of the Börjeson-Forssman-Lehmann syndrome in males and heterozygous females with PHF6 mutations. *Clin. Genet.* **65,** 226–232
4. Van Vlierberghe, P., Palomero, T., Khiabanian, H., Van der Meulen, J., Castillo, M., Van Roy, N., De Moerloose, B., Philippé, J., Gonzalez-Garcia, S., Toribio, M. L., Taghon, T., Zuurbier, L., Cauwelier, B., Harrison, C. J., Schwab, C., Pisecker, M., Strehl, S., Langerak, A. W., Gecz, J., Sonneveld, E., Pieters, R., Paietta, E., Rowe, J. M., Wiernik, P. H., Benoit, Y., Soulier, J., Poppe, B., Yao, X., Cordon-Cardo, C., Meijerink, J., Rabadan, R., Speleman, F., and Ferrando, A. (2010) PHF6 mutations in T-cell acute lymphoblastic leukemia. *Nat. Genet.* **42,** 338–342
5. Chao, M. M., Todd, M. A., Kontny, U., Neas, K., Sullivan, M. J., Hunter, A. G., Picketts, D. J., and Kratz, C. P. (2010) T-cell acute lymphoblastic leukemia in association with Börjeson-Forssman-Lehmann syndrome due to a mutation in PHF6. *Pediatr. Blood Cancer* **55,** 722–724
6. Van Vlierberghe, P., Patel, J., Abdel-Wahab, O., Lobry, C., Hedvat, C. V., Balbin, M., Nicolas, C., Payer, A. R., Fernandez, H. F., Tallman, M. S., Paietta, E., Melnick, A., Vandenberghe, P., Speleman, F., Aifantis, I., Cools, J., Levine, R., and Ferrando, A. (2011) PHF6 mutations in adult acute myeloid leukemia. *Leukemia* **25,** 130–134
7. Feng, W., Yonezawa, M., Ye, J., Jenuwein, T., and Grummt, I. (2010) PHF8 activates transcription of rRNA genes through H3K4me3 binding and H3K9me1/2 demethylation. *Nat. Struct. Mol. Biol.* **17,** 445–450
8. Kleine-Kohlbrecher, D., Christensen, J., Vandamme, J., Abarrategui, I., Bak, M., Tommerup, N., Shi, X., Gozani, O., Rappsilber, J., Salcini, A. E., and Helin, K. (2010) A functional link between the histone demethylase PHF8 and the transcription factor ZNF711 in X-linked mental retardation. *Mol. Cell* **38,** 165–178
9. Liu, W., Tanasa, B., Tyurina, O. V., Zhou, T. Y., Gassmann, R., Liu, W. T., Ohgi, K. A., Benner, C., Garcia-Bassets, I., Aggarwal, A. K., Desai, A., Dorrestein, P. C., Glass, C. K., and Rosenfeld, M. G. (2010) PHF8 mediates histone H4 lysine 20 demethylation events involved in cell cycle progression. *Nature* **466,** 508–512
10. Peña, P. V., Davrazou, F., Shi, X., Walter, K. L., Verkhusha, V. V., Gozani, O., Zhao, R., and Kutateladze, T. G. (2006) Molecular mechanism of histone H3K4me3 recognition by plant homeodomain of ING2. *Nature* **442,** 100–103
11. Qi, H. H., Sarkissian, M., Hu, G. Q., Wang, Z., Bhattacharjee, A., Gordon, D. B., Gonzales, M., Lan, F., Ongusaha, P. P., Huarte, M., Yaghi, N. K., Lim, H., Garcia, B. A., Brizuela, L., Zhao, K., Roberts, T. M., and Shi, Y. (2010) Histone H4K20/H3K9 demethylase PHF8 regulates zebrafish brain and craniofacial development. *Nature* **466,** 503–507
12. Shi, X., Hong, T., Walter, K. L., Ewalt, M., Michishita, E., Hung, T., Carney, D., Peña, P., Lan, F., Kaadige, M. R., Lacoste, N., Cayrou, C., Davrazou, F., Saha, A., Cairns, B. R., Ayer, D. E., Kutateladze, T. G., Shi, Y., Côté, J., Chua, K. F., and Gozani, O. (2006) ING2 PHD domain links histone H3 lysine 4 methylation to active gene repression. *Nature* **442,** 96–99
13. Pierce, A. J., Hu, P., Han, M., Ellis, N., and Jasin, M. (2001) Ku DNA end-binding protein modulates homologous repair of double-strand breaks in mammalian cells. *Genes Dev.* **15,** 3237–3242
14. Gong, Z., Cho, Y. W., Kim, J. E., Ge, K., and Chen, J. (2009) Accumulation of Pax2 transactivation domain interaction protein (PTIP) at sites of DNA breaks via RNF8-dependent pathway is required for cell survival after DNA damage. *J. Biol. Chem.* **284,** 7284–7293
15. Kruhlak, M., Crouch, E. E., Orlov, M., Montaño, C., Gorski, S. A., Nussenzweig, A., Misteli, T., Phair, R. D., and Casellas, R. (2007) The ATM repair pathway inhibits RNA polymerase I transcription in response to chromosome breaks. *Nature* **447,** 730–734
16. Aris, J. P., and Blobel, G. (1991) cDNA cloning and sequencing of human fibrillarin, a conserved nucleolar protein recognized by autoimmune antisera. *Proc. Natl. Acad. Sci. U.S.A.* **88,** 931–935
17. Schultz, A., Nottrott, S., Watkins, N. J., and Lührmann, R. (2006) Protein-protein and protein-RNA contacts both contribute to the 15.5K-mediated assembly of the U4/U6 snRNP and the box C/D snoRNPs. *Mol. Cell Biol.* **26,** 5146–5154
18. Lazzaro, F., Novarina, D., Amara, F., Watt, D. L., Stone, J. E., Costanzo, V., Burgers, P. M., Kunkel, T. A., Plevani, P., and Muzi-Falconi, M. (2012) RNase H and postreplication repair protect cells from ribonucleotides incorporated in DNA. *Mol. Cell* **45,** 99–110
19. Wahba, L., Amon, J. D., Koshland, D., and Vuica-Ross, M. (2011) RNase H and multiple RNA biogenesis factors cooperate to prevent RNA:DNA hybrids from generating genome instability. *Mol. Cell* **44,** 978–988
20. Donati, G., Bertoni, S., Brighenti, E., Vici, M., Treré, D., Volarevic, S., Montanaro, L., and Derenzini, M. (2011) The balance between rRNA and ribosomal protein synthesis up- and downregulates the tumour suppressor p53 in mammalian cells. *Oncogene* **30,** 3274–3288